A model for Quick Load Analysis for monopile-type offshore wind turbine substructures

Signe Schløer[1], Laura Garcia Castillo[2], Morten Fejerskov[2], Emanuel Stroescu[2], and Henrik Bredmose[1]

[1]The Technical University of Denmark, Nils Koppels Allé, Building. 403, DK-2800 Kgs. Lyngby, Denmark. [2] Universal Foundation, Langerak 17, DK-9220 Aalborg Øst, Denmark

E-mail: sigs@dtu.dk

Abstract. A model for Quick Load Analysis, QuLA, of an offshore wind turbine substructure is presented. The aerodynamic rotor loads and damping are precomputed for a load-based configuration. The dynamic structural response is represented by the first global fore-aft mode only and is computed in the frequency domain using the equation of motion. The model is compared against the state of the art aeroelastic code, Flex5, and both life time fatigue and extreme loads are considered in the comparison. In general there is good similarity between the two models. Some derivation for the sectional forces are explained in terms of the model simplifications. The difference in the sectional moments are found to be within 14% for the fatigue load case and 10% for the extreme load condition.

1. Introduction

In order to ensure cost-efficient offshore wind farms, it is necessary to optimize the design. Particularly the substructures are expensive and can, according to [1] , account for 20 % of the total cost of energy.

It is often different parties who design the substructure and the wind turbine of an offshore wind turbine. The iteration process where the design suppliers of the wind turbine and the substructure send design loads back and forth slows the design process down. The process is already time-consuming since extensive load-case simulations have to be made where different wind speeds and wave climates are combined. If instead a fully integrated simulation of the foundation and wind turbine is used, the design process will be faster and the number of uncertainties in the design will be reduced. In the preliminary design phase, the integrated simulation and optimization can be accelerated further with a simplified description of the loading from wind and waves and a simple but fast dynamic model. This allows for optimization of the foundation in an early stage of the design.

In the present paper a model for **Qu**ick **L**oad **A**nalysis, QuLA, is presented. This is a fast model for calculation of dynamic loads of an offshore wind turbine tower and foundation. In the present paper the foundation is bottom fixed, however QuLA has been applied to a floating wind turbine too, see [3] for preliminary results. The 10MW DTU reference wind turbine [2] is considered and the foundation is the Mono Bucket foundation of Universal Foundation (http://universal-foundation.com/). The Mono Bucket consists of a shaft and a bucket as shown in figure 1. Compared to a monopile, the Mono Bucket has the advantage of very small noise

impact during installation, reduced scour protection, and no need for a transition piece. So far a Vestas V90-3.0 MW offshore wind turbine has been erected on a Mono Bucket foundation in November 2002 in Frederikshavn harbour, Denmark. Besides, a met mast foundation for the Horns Rev 2 site was installed in March 2009 and decommissioned successfully in 2015, and two other met mast foundations were installed at Forewind's Dogger Bank offshore wind site in September 2013. In order to make the Mono Bucket foundation commercial an industrialization and production evolution is needed. A fast numerical model to calculate the dynamic loads of the foundation is one of the tools applied in that process.

This paper investigates how well QuLA performs by comparing the model against the aeroelastic code Flex5, [4]. The sectional inline force and overturning moment in different sections in the Mono Bucket and tower are considered for two load cases and both life time fatigue and extreme loads are analysed. The largest difference of 30% are found for the sectional inline force in the bottom of the Mono Bucket foundation, while the overturning moments compare well in most parts of the tower and Mono Bucket foundation with the largest difference being 14% . The design of the Mono Bucket foundation is confidential. Therefore, in this paper the results of the sectional forces and moments and response spectra are presented in normalized form.

2. The numerical model, QuLA

In QuLA, only the Mono Bucket foundation and wind turbine tower are considered and described as a simple Euler beam. On top of the beam a top mass, M_{top}, representing the rotor and nacelle is added. The top mass is placed in same height as the center of mass in the nacelle, x_N, 2.75 m above the tower top, X_{TT}, as illustrated in figure 2. The foundation is only considered down to the sea bed and the stiffness of the soil and lid and skirt of the bucket is described by a coupled translational and rotational spring, K_s. The dynamic structural response is represented by the first natural mode only and the equation of motion is solved in the frequency domain.

The philosophy behind the model is to pre-calculate the aerodynamic forces in an aeroelastic model with a stiff foundation and tower for all considered wind speeds. Also the aerodynamic damping is pre-calculated in Flex5 by decay tests for all considered wind speeds. The aerodynamic forces and damping are subsequently reused several times in QuLA for different tower and substructure configurations.

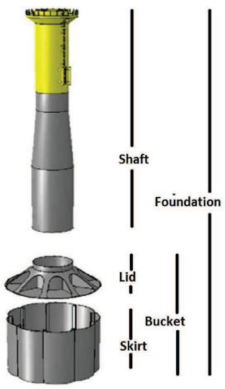

Figure 1: Mono Bucket foundation.

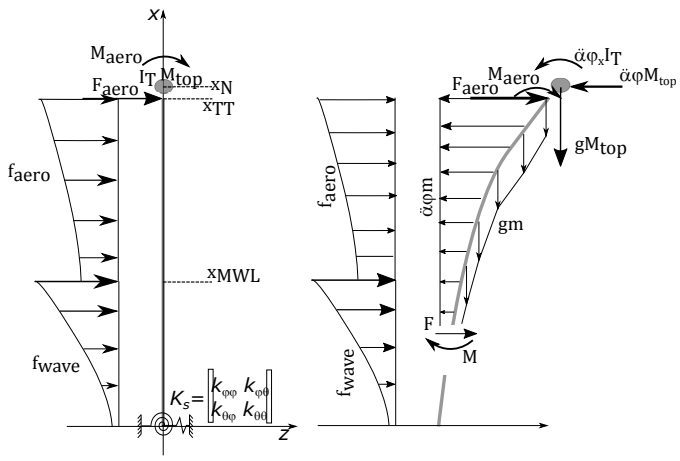

Figure 2: Left: Sketch of the beam and the external forces. Right: The external and internal forces which contribute to sectional force, F, and moment, M.

2.1. The external forces

The external forces are the distributed wave force and the turbulent wind force as seen in figure 2. The pre-calculated rotor shaft loads are applied as a time varying point force, F_{aero} and overturning moment, M_{aero} at the top of the tower. The aerodynamic damping is added to the equation of motion as a viscous linear damping force, where the damping coefficient is a function of the mean wind speed. The dependency to turbulence intensity of the damping was investigated, but not found to be important. The force from the wind on the tower is also included and is calculated inside QuLA by the power law from IEC61400-3 [5]

$$f_{tower}(x,t) = \frac{1}{2}\rho_a C_{Da} D \left(\left(\frac{x}{x_n} \right)^{\lambda} W(t) \right)^2, \tag{1}$$

with $\lambda = 0.14$ in load case 1.2 and $\lambda = 0.11$ in load case 6.1. Here $\rho_a = 1.225$ kg/m^3 is the density of air, $C_{Da} = 0.6$ is the drag coefficient, $D(x)$ is the diameter of the tower and W is the turbulent wind speed at the nacelle.

The wave kinematics and hydrodynamic force are also calculated inside QuLA. To enable fast calculations of the structural response no stretching of the wave kinematics is applied and the wave kinematics are therefore only defined up to still water level, SWL.

In situations where fatigue loads are considered, linear wave theory is often sufficient to describe the wave kinematics, [6]. An irregular wave realization is characterised by the significant wave height H_s and the peak wave period T_p. The linear irregular wave kinematics are calculated in the frequency domain and afterwards transformed to the time domain using inverse Fast Fourier transformation. The distributed hydrodynamic load on the structure is calculated by Morison's equation

$$f_{wave}(x,t) = \rho C_m A \dot{u} + \rho A \dot{u} + \frac{1}{2}\rho C_D D u|u| \tag{2}$$

Here $\rho = 1025$ kg/m^3 is the density of water, $A(x)$ is the cross sectional area of the pile and $D(x)$ is the diameter of the pile. The horizontal particle velocity and acceleration are denoted u and $\dot{u} = \frac{du}{dt}$. The coefficients, C_D and C_m, are the drag and added mass coefficients, with $C_M = 1 + C_m$ being the inertia coefficient. The coefficients are functions of the Keulegan-Carpenter number, KC, and Reynolds number, Re, and are calculated following the recommendations in [7]. For irregular wave realizations KC and Re can, according to [8], be calculated from the standard deviation of the horizontal velocity at still water level and the mean wave period.

The hydrodynamic damping due to the structural motion is considered small and neglected. Therefore, it is not the relative accelerations and the relative velocities, which are considered in the added mass and drag force, first and third term in (2), respectively.

The added mass coefficient, C_m, is corrected for diffraction effects by the theory of MacCamy-Fuchs, [9], which is valid for linear waves. The correction is important for waves with $D/L > 0.2$, where L is the wave length. In a water depth of 50m it corresponds to wave frequencies larger than approximately $f > 0.19$ Hz. To include the diffraction effect, the added mass force is calculated in the frequency domain and afterwards transformed to the time domain.

In order to simultaneously include both the effect of wave irregularity and wave nonlinearity in the structural analysis, IEC61400-3 [5] suggests to embed a large nonlinear stream function wave in the linear irregular wave time series to represent extreme waves. This is done in situations where ultimate loads (ULS) are considered. Following the work of Rainey, [10] and [11], the Morison's equation is extended by the axial divergence correction term

$$f_{Rainey}(x,t) = \rho A C_m w_x u, \tag{3}$$

which according to Manners and Rainey, [12], corrects for the assumption that the cylinder is slender in the vertical direction. Here the vertical particle velocity is denoted w and index "x" means that the variable is differentiated with respect to x.

Finally a point force should according to Rainey [11] be added at the intersection with the water level

$$F_s(t) = -\frac{1}{2}\rho A C_m \eta_z u^2. \tag{4}$$

Here η_z is the slope of the free surface elevation and represents the change of the free surface elevation along the pile-diameter. This force can be seen as a slamming force.

The Rainey terms, (3) and (4), are nonlinear contributions to the Morison force and therefore they should only be added to the Morison's equation (2) in situations where a nonlinear single wave event is embedded in the irregular linear wave realization in the ULS-analysis.

2.2. The structural model

The structural dynamic deflection of the Mono Bucket and tower, u, is represented by a shape function, φ and a generalized coordinate α as $\mathrm{u} = \alpha(t)\varphi(x)$. Shape functions are often introduced when the equation of motion of a system is solved to decrease the number of degrees of freedom in the system and thereby the computational time. Only one shape function is considered in QuLA. While this may not provide an accurate representation of the full deformation, it is here used for the purpose of approximating the associated inertia loads for the sectional forces, see (13)-(14). The shape function and the natural angular frequency, ω_0 are found by considering a standard eigenvalue problem,

$$\mathbf{M}\ddot{\alpha}\underline{\varphi} + \mathbf{K}\alpha\underline{\varphi} = 0, \quad \text{where} \quad \alpha = \exp(i\omega_0 t) \Leftrightarrow \tag{5a}$$

$$-\mathbf{M}\omega_0^2\underline{\varphi} + \mathbf{K}\underline{\varphi} = 0 \Rightarrow \omega_0^2\underline{\varphi} = \mathbf{M}^{-1}\mathbf{K}\underline{\varphi}. \tag{5b}$$

The stiffness and mass matrix is calculated by the finite element method. Stiffness elements representing the stiffness from the soil-structure interaction, K_s in figure 2, is calculated in the geotechnical software tool Plaxis, [14] and is added to the stiffness matrix in the bottom of the pile. The top mass and mass moment of inertia around the nacelle (y-axis), I_T, are added to the mass matrix in the top of the pile. To get the correct first natural frequency it is important to define M_{top} and I_T in same height as the center of mass in the nacelle, x_N.

The structural dynamics are calculated by the equation of motion

$$\ddot{\alpha}GM + \alpha GK + \dot{\alpha}GD = GF. \tag{6}$$

In order for the model to be fast the equation of motion is solved in frequency domain, since the solution α can then be solved at once for all time steps. In frequency domain the generalized coordinate can be expressed as

$$\alpha = \sum_{j=1}^{N_f} \hat{\alpha}_j \exp(i\omega_j t) + c.c., \tag{7}$$

where ω_j is the smallest angular frequency in the time series and $c.c.$ is the complex conjugate. The equation of motion

$$-\omega^2 GM\hat{\alpha} + i\omega GD\hat{\alpha} + GK\hat{\alpha} = GF \Leftrightarrow \hat{\alpha} = \frac{\hat{GF}}{-\omega^2 GM + i\omega GD + GK} \tag{8}$$

then solves the linear response in frequency domain and can readily be transposed to the time domain by inverse FFT.

The generalized mass, GM, and stiffness, GK, can be obtained from (5a) by left-multiplication of φ^{T} or are given as

$$GM = \int_{x=0}^{x_{TT}} m\varphi(x)^2\,dx + M_{top}\varphi(x_n)^2 + I_T\varphi_x(x_N)^2, \tag{9}$$

$$GK = \int_{x=0}^{x_{TT}} EI\varphi_{xx}(x)^2\,dx. \tag{10}$$

Here $m(x)$ is the distributed mass of the tower and Mono Bucket foundation, φ_x is the angular deflection of the shape function and φ_{xx} is the curvature of the shape function. The stiffness factor is given by the modulus of elasticity, E, and the moment of inertia I. Further, the damping, GD, and force, GF, are given as

$$GD = \zeta\frac{2GK}{\omega_0} + D_{aero}, \tag{11}$$

$$GF = \int_{x=0}^{x_{MWL}} \varphi f_{wave}dx + F_s + F_{aero}\varphi(x_{TT}) + M_{aero}\varphi_x(x_{TT}) + \int_{x_{MWL}}^{x_{TT}} \varphi f_{tower}dx, \tag{12}$$

The damping ζ is the damping ratio representing structural damping, soil damping and hydrodynamic radiation damping.

After the equation of motion is solved, the sectional forces and moments can be calculated. The external and internal forces, which contribute to the sectional forces and moments are shown in figure 2 and the forces and moments are calculated as

$$\begin{aligned} F(x^*,t) = &-\ddot{\alpha}\int_{x^*}^{x_{TT}} m\varphi(x)dx - \ddot{\alpha}M_{top}\varphi(x_N) + \int_{x^*}^{x_{MWL}} f_{wave}dx + F_s + F_{aero} \\ &+ \int_{x^*}^{x_{TT}} f_{tower}dx + \alpha g M_{top}\varphi_x(x_N) + \alpha g\int_{x^*}^{x_{TT}} m\varphi_x(x)dx \end{aligned} \tag{13}$$

$$\begin{aligned} M(x^*,t) = &-\ddot{\alpha}\int_{x^*}^{x_{TT}} m\varphi(x)[x-x^*]dx - \ddot{\alpha}M_{top}\varphi(x_N)[x_n-x^*] - \ddot{\alpha}I_T\varphi_x(x_N) \\ &+ \int_{x^*}^{x_{MWL}} f_{wave}[x-x^*]dx + F_s[x_{MWL}-x^*] + M_{aero} + F_{aero}[x_{TT}-x^*] \\ &+ \int_{x^*}^{x_{TT}} f_{aero}[x-x^*]dx + \alpha M_{top}g[\varphi(x_N)-\varphi(x^*)] + \alpha g\int_{x^*}^{x_{TT}} m[\varphi(x_{TT})-\varphi(x)]dx, \end{aligned} \tag{14}$$

where g is the gravity. The first two terms in both equations are the contribution from the dynamics of the structure. When the equation of motion is solved the Mono Bucket and tower

are treated as an Euler beam, where the deflections are assumed small and only lateral loads are considered. Second-order contributions from the bending of the beam are therefore neglected in the solution in order for the model to be fast. However, in the sectional forces and moment the contribution from gravity due to the bending of the beam is included as stated in the last two terms in both equations. While this approach thus represent a difference in the forces applied for dynamics and sectional loads, it was found to improve the sectional loads.

3. Metocean data and structure

The load cases in the present analysis are based on the metocean data from the artificial site "'K13 Deepwater Site"' from the Upwind-project [13]. The water depth is $h = 50\,\mathrm{m}$. Two load cases are studied, load case 1.2 which consider the fatigue limit state (FLS) and load case 6.1 which consider the ultimate limit state (ULS). The time series of each wind and sea state is 1 hour long which corresponds to six seeds of 600 s. In load case 1.2 the wind turbine operates, and the wind speed ranges from 4m/s to 25 m/s with an interval of 2m/s. The wind speeds and the corresponding probability of occurrence, P_r, turbulence intensity, I, sea states and damping due to the wind, D_{aero}, are stated in table 1.

In load case 6.1 the wind turbine is parked and the wind speed is 44.03 m/s. The corresponding sea state has a significant wave height of $H_s = 9.40\mathrm{m}$ and a peak period of $T_p = 10.87\mathrm{s}$. First a irregular linear wave time series is created. For every 600 s the largest wave in the interval is replaced with a nonlinear regular stream function wave with a wave height of $H = 1.86H_S = 17.48\mathrm{m}$, [5]. The corresponding wave period should be chosen as the period in the interval $11.1\sqrt{H_s/g} < T < 14.3\sqrt{H_s/g}$, [5], which results in the largest load. For the present structure that is $T = 11.1\sqrt{H_s/g} = 10.87\mathrm{s}$.

The wind turbine is the 10 MW DTU reference wind turbine, [2]. The first natural frequency of the structure is in between the 1P and 3P frequency interval of the wind turbine (1P=0.115–0.159 Hz). The Mono Bucket foundation is designed to withstand the extreme static forces stated in the report of the DTU 10 MW wind turbine [2]. In both Flex5 and QuLA a logarithmic damping of $\delta = 2\pi\zeta = 6\%$ is included as viscous damping to represent soil damping, structural damping of the Mono Bucket and tower and hydrodynamic radiation damping.

4. Results

In order for QuLA to be a useful tool in the design-process, the model has to be faster than a more advanced aeroelastic model. Before QuLA can be used it is necessary to precalculate the stochastic point loads, F_{aero} and M_{aero} and the aerodynamic damping. Though, once they are calculated they can be used repeatedly in the design process.

To calculate a single wind and sea state on a Microsoft Windows machine with a clock rate of 2.30 GHz QuLA is 40 times faster than Flex5, while on a Linux cluster machine with a clock rate of 1.9 GHz QuLA is 3.3 times faster. It is belived that this can be speeded up to similar performance as at the Windows machine. QuLA is further parallelised, and can on a HPC-cluster calculate in parallel all 11 wind and sea states of load case 1.2 in approximately 45s.

4.1. Shape function and eigenfrequency

The complete shape function of both the tower and bucket foundation in Flex5 is compared to the shape function of QuLA in figure 3. The shape functions are close to being identical. The deviation between the first natural frequency of the two models is 1%. The difference is caused by differences in the models: In Flex5 the gravity's contribution to the bending of the pile is included in the equation of motion, which gives a larger moment of inertia and therefore a smaller frequency. In QuLA the contribution of the gravity is only included in the sectional forces calculated after the equation of motion is solved.

4.2. Fatigue limit state

Load case 1.2 considers the fatigue limit state during operation. In fatigue analysis, equivalent loads, L_{eq}, can be used as a reference loading and represents one load range value that for a certain number of cycles, $N_{eq} = 10 \cdot 10^6$, results in the same damage level as the history of investigated fatigue loads. It is calculated as

$$L_{eq} = \left(\sum_j \left(\sum_i \frac{N_{s,i} S_i^{\mathrm{m}}}{N_{eq}} \right) P_{r,j} \right)^{\frac{1}{\mathrm{m}}} \tag{15}$$

Here $N_{s,i}$ is the number of occurrences of each stress range, S_i, for the considered wind and sea state, j. The equivalent loads are calculated for the sectional forces and moments using a Wöhler exponent of m = 4 and taking the wind and sea states probability of occurrence into account.

V (m/s)	P_r (-)	I (-)	H_S (m)	T_p (s)	D_{aero} (kg/s)
4.16	0.11	0.29	1.10	5.88	720
6.23	0.14	0.23	1.18	5.76	720
8.31	0.16	0.20	1.31	5.67	810
10.39	0.15	0.18	1.48	5.74	990
12.47	0.13	0.17	1.70	5.88	2160
14.55	0.11	0.16	1.91	6.07	2700
16.62	0.08	0.15	2.19	6.37	2250
18.70	0.05	0.15	2.47	6.71	1890
20.78	0.03	0.14	2.76	6.99	1530
22.56	0.02	0.14	3.09	7.40	1350
24.94	0.01	0.14	3.42	7.80	1260

Table 1: The wind speeds and the corresponding probability of occurrence, turbulence intensity, sea states and aerodynamic damping ratios for load case 1.2.

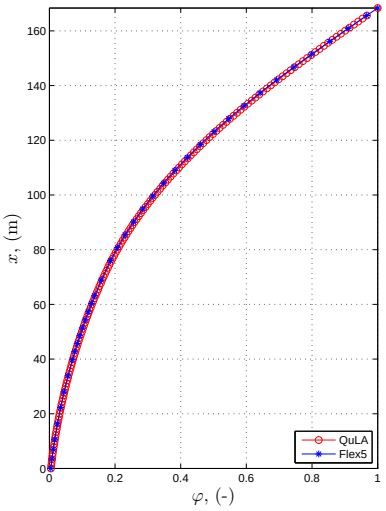

Figure 3: The shape function.

In figure 4 the ratio of the equivalent forces and moments of QuLA to those of Flex5 (QuLA/Flex5) throughout the tower and Mono Bucket are shown. In the tower, both the equivalent forces and moments in QuLA are largest with a ratio of approximately 1.12. In the Mono Bucket the equivalent forces are largest in Flex5, and the difference between the two models increases down through the Mono Bucket. Near the sea bed the ratio between the equivalent forces of QuLA to those of FLex5 is 0.72. This change from the tower to the monopile can be explained by considering a sequence of the time series and response amplitude spectra of the 1 hour time series of the sectional forces at the intersection between the Mono Bucket foundation and tower (26 m above MWL) and at the sea bed as seen in figures 5-6. The forces are based on the wind and sea state with a wind speed of 10.39m/s, since this is found to contribute the most to the equivalent loads.

The energy around the first natural frequency is captured well by QuLA. However, the forces contain more energy compared to Flex5, which suggests that the aerodynamic damping is a little too small in QuLA. Using Flex5 a big amount of energy is also found at the second natural frequency of the tower and Mono Bucket - in particular at the sea bed. Since QuLA only have one degree of freedom, no energy is observed in QuLA at this frequency. The main part of the modal energy of the second natural frequency is distributed in the Mono Bucket, which explains why the difference between the two models at the second natural frequency is largest at the sea bed and why the ratio of the equivalent forces in figure 4 decreases thoughout the Mono Bucket.

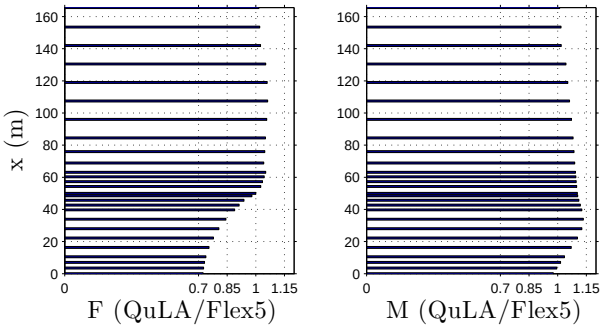

Figure 4: The ratio of the equivalent loads of QuLA to those of Flex5 in all sections in the tower and Mono Bucket.

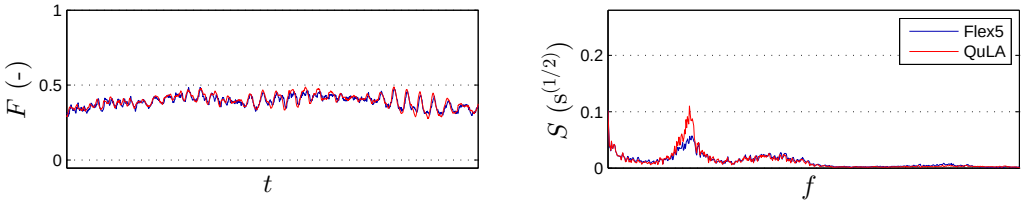

Figure 5: Sectional force 26 m above MWL.

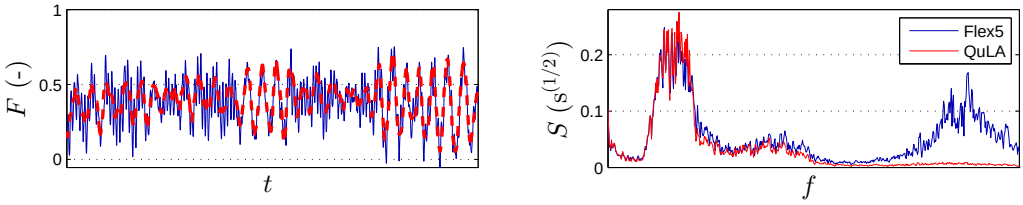

Figure 6: Sectional force at sea bed.

QuLA has the largest equivalent moment in all sections, figure 4, with a ratio 1.08 to those of Flex5. The difference increases until approximately 20 m above the sea bed after which the equivalent moments in Flex5 become larger relative to those in QuLA. The reason there is such a difference between the equivalent forces and moments is that the moments not only depend on the size of the overlying forces but also on the size of the moment arm.

Instead of the equivalent load ratio the damage ratio could also be considered which differs from the equivalent load ratio by the power of the Wöhler exponent, m. Thus, the difference between the models is larger with that measure.

4.3. Ultimate limit state

Load case 6.1 considers a storm condition and therefore ULS. The wind turbine is parked, and the aerodynamic force and damping are therefore small. The contribution from the wave force is therefore expected to be significant.

In figure 7 the probability of exceedance, P, of the positive peaks in the 1 hour time series of the sectional forces and moments in five sections of the Mono Bucket and tower are shown.

QuLA has the largest force peaks for high probability of exceedance while Flex5 has the largest force peaks for low probability of exceedance, however in the tower the probability of the force peaks are quite equal. At MWL there is a large difference between the curves of the two models, in particular for $P < 0.03$. The peaks of Flex5 is largest, which is caused by the Wheeler

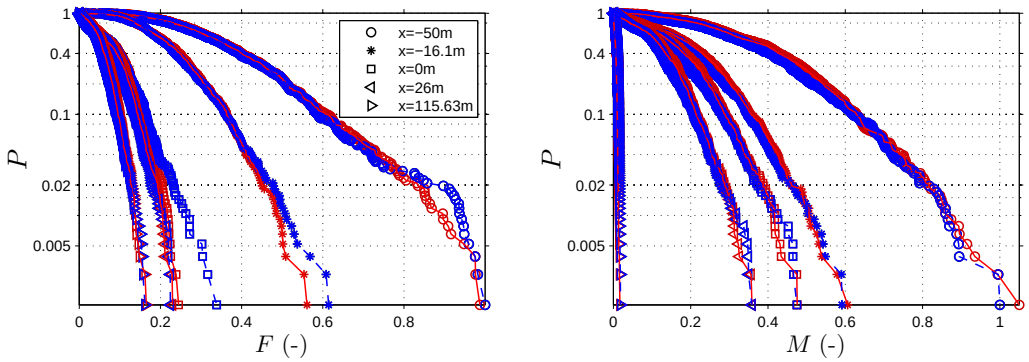

Figure 7: Probability of exeedance of the positive peaks in the time series of the sectional forces and moments. Blue: Flex5. Red: QuLA

stretching in Flex5, which stretches the wave kinematics up to the free surface elevation instead of only being defined to MWL as in QuLA. In the Mono Bucket 26 m above the sea bed, the difference between the two models is still significant but smaller. At the sea bed the force-curves of the two models are again quite equal. The three largest force peaks are very close to each other.

The probability curves of the moments of the two models are more equal in all five sections. Particularly the largest moments, which are important in ULS, compare well. To compare the dynamics of the two models a sequence of the time series and response amplitude spectra of the 1 hour time series of the sectional forces and moments at the intersection between the tower and Mono Bucket and at the sea bed are considered, figures 8-9. In the tower, the energy of the force and moment is located around the first natural frequency, however QuLA contains more energy at this frequency. In the time series, the response dampens faster in Flex5. At the sea bed, the energy is located both at the wave peak frequency and at the first natural frequency. The energy distribution of the force is very similar in the two models, while for the moments QuLA contains most energy. In the time series the forces of the two models are very similar when a stream function wave is embedded into the wave realization - indicated with an arrow in the figure. However, for the chosen sequence of the time series the moments are not largest when the stream function wave is embedded. Instead the moments are largest in the beginning of the time sequence where the wave kinematics are described by linear wave theory. This means that for the stiffness and natural frequency of this foundation, the linear wave kinematics can also result in the largest moments. In other part of time series, though, the embedded stream function wave results in the largest overturning moment at the sea bed. Still, this shows that the dynamic forces caused by the structural motion - and not only the static forces, are important in ULS.

To calculate the ultimate loads the 1 hour time series of the forces and moments are divided into 6x600s intervals. In each interval the largest load is found. The ultimate load is the average of these six loads. The ratios of the ultimate loads of QuLA to those of Flex5 are seen in figure 10. In the top of the tower the ultimate sectional forces in Flex5 are largest with a ratio of 0.95 while just above MWL the two models result in the same ultimate sectional force. Around MWL there is an increase in the difference between the two models and the ratio of the ultimate sectional forces of QuLA to those of Flex5 reduces to 0.7. This is due to Wheeler stretching not applied in QuLA. However, the difference between the models decreases down through the Mono Bucket and at the sea bed the models are very close to each other with a ratio of 0.99. This is expected, since the wave force in load case 6.1 is the largest contributor to the sectional force, and the force at the seabed are the sum of the distributed force, which is calculated in

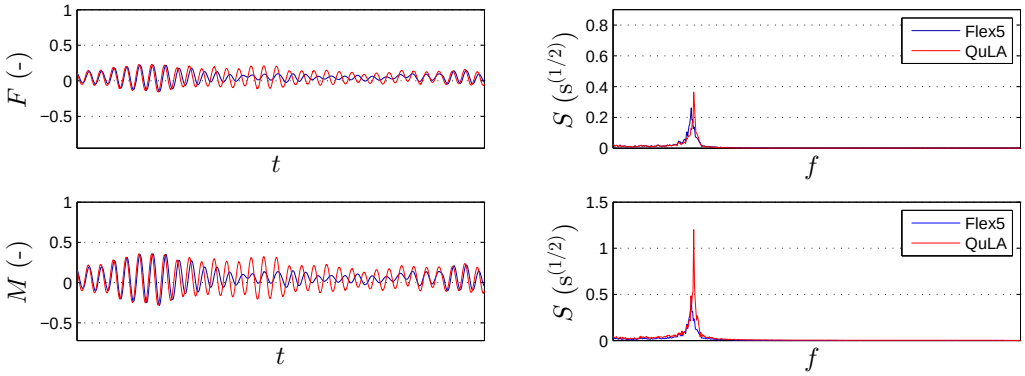

Figure 8: Sectional force and moment 26 m above MWL.

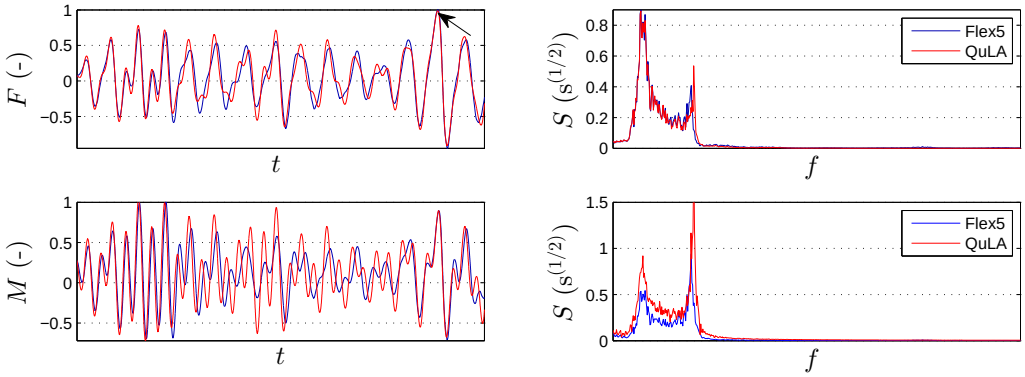

Figure 9: Sectional force and moment at sea bed.

same way in the two models, though not distributed equally.

With a ratio of approximately 0.95 the difference between the ultimate sectional moments of the two models is more or less constant in all sections in the tower, with those of QuLA being smallest. In the Mono Bucket the difference between the two models decreases and at the sea bed the ratio is only 0.99.

5. Conclusion

A model, QuLA, to make fast linear response calculations of the foundation and tower of an offshore wind turbine has been presented. The model solves the equation of motion in the frequency domain and uses precalculated aerodynamic forces and damping as function of the wind speed.

The shape function and the first natural frequency of the two models are very close to be identical. In the fatigue analysis for the tower, the ratio of the equivalent forces of QuLA to those of Flex5 was found to be 1.12, while the excitation of the second structural frequency in Flex5 results in larger difference in the Mono Bucket. At the sea bed the equivalent forces of QuLA are smallest with a ratio of 0.7. Considering the equivalent moments, which is often more important, QuLA results in the largest values throughout the tower and Mono Bucket with a ratio of approximately 1.1 to those of Flex5.

In the ultimate load analysis, both the ultimate forces and moments of QuLA are smallest in all sections with a ratio of approximately 0.95-0.99 to those of Flex5 in most sections. This difference is due to differences in the dynamic response of the two models and shows that for

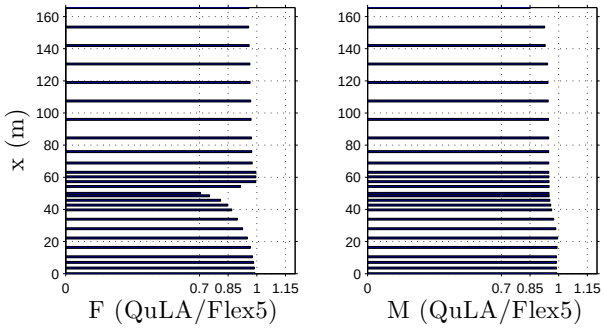

Figure 10: The ratio of the ultimate loads of QuLA to those of Flex5 in all sections in the tower and Mono Bucket.

ULS not only the extreme waves but also the dynamics of the structure is important. At MWL, though, the missing Wheeler stretching in QuLA, results in much smaller ultimate forces. This difference could be improved by including Wheeler stretching in the model, which though would decrease the computational speed of the model.

The proposed model of this paper presents a fast model with good accuracy, especially for the sectional moments. The analysis indicates that in the early stage of the design phase a simple dynamic model can be used in the iterative process to make a preliminary design of the foundation and wind turbine tower. After this, a full aeroelastic model can be used to verify the design and optimize it further. Combined use of a fast and an accurate model might even be applied to enhance this optimization further.

References

[1] Krohn S, Awerbuch S and Morthorst P E 2009 *The economics of wind energy* (European Wind Energy Association)
[2] Bak C, Zahle F, Bitsche R, Kim T, Yde A, Henriksen L, Natarajan A and Hansen M 2013 Description of the DTU 10 MW Reference Wind Turbine Tech. rep. DTU Wind Energy
[3] Lemmer F, Müller K, Pegalajar-Jurado A, Borg M and Bredmose H 2015 Qualification of innovative floating substructures for 10mw wind turbines and water depths greater than 50m Tech. rep. LIFES50+
[4] Øye S 1996 *28th IEA Meeting of Experts Concerning State of the Art of Aeroelastic Codes for Wind Turbine Calculationsn (available through International Energy Agency)*
[5] IEC61400-3 2009 *International Standard. Wind turbines – Part 3: Design requirements for offshore wind turbines* 1st ed
[6] Schløer S, Bredmose H and Bingham H 2016 The influence of fully nonlinear wave forces on aero-hydro-elastic calculations of monopile wind turbines manuscript submitted for publication
[7] DNV-OS-J101 2010 *Design of Offshore Wind Turbines* (Det Norske Veritas)
[8] Sumer M and Fredsøe J 2006 *Hydrodynamics around cylindrical structures* (World Scientific Publishing Co. Pte. Ltd.) ISBN 981-270-039-0
[9] MacCamy R and Fuchs R 1954 Wave forces on piles: A diffraction theory Tech. rep. U.S. Army Corps of Engineering, Beach Erosion Board, Tech. Memo. No. 69
[10] Rainey R 1989 *Journal of Fluid Mechanics* **204** 295–324
[11] Rainey R 1995 *Proceedings of the Royal Society of London. Series A: Mathematical and Physical Sciences* **450** 391–416
[12] Manners W and Rainey R 1992 *Proceedings of the Royal Society of London. Series A: Mathematical and Physical Sciences* **436** 13–32
[13] Fischer T, de Vries W and Schmidt B 2010 Upwind Design Basis. WP4: Offshore Foundations and Support Structures Tech. rep. Project UpWind Allmandring 5B, 70550 Stuttgart, Germany
[14] Brinkgreve R, Kumarswamy S and Swolfs W 2016 Plaxis 2016 Tech. rep. Plaxis bv